

A Study of the Optimization and Characterization of Friction Stir Welded AA5083 and AA6082

Mullaiarasu R.¹ , Thilagham K. T.², Noorullah D.³

¹PG Scholar, Department of Metallurgical Engineering, Government College of Engineering, Salem, Tamilnadu, India.

²Assistant Professor, Department of Metallurgical Engineering, Government College of Engineering, Salem, Tamilnadu, India

³Head of the Department, Department of Metallurgical Engineering, Government College of Engineering, Salem, Tamilnadu, India

Email: mullaiarasu389@gmail.com

Article History

Received: 26 May 2021

Accepted: 24 June 2021

Keywords:

Friction Stir Welding;
Optimized;
Taguchi L9 Orthogonal;
Dissimilar Plates;
Travel Speed

Abstract

The joining of dissimilar 6mm thickness plates of AA6082 & AA5083 was carried out using friction stir welding (FSW) technique. The process parameters are optimized using Taguchi L9 orthogonal design of experiments. Where the rotational speed (600, 900, 1200 rpm), travel speed (60, 90, 120 mm/min), and tilt angle (0, 1, 2°) were the parameters taken into consideration. The optimum process parameters were determined with the reference to tensile strength, yield stress, elongation of the joint. Friction stir welding of aluminium alloys has gained popularity in manufacturing industries such as ship building, aircraft production, railways and automotive. Effect of process parameter on tensile properties, microstructure, and hardness distribution of the welded joints were investigated.

1. Introduction

Friction stir welding has seen significant advancements and improvements in light weight construction. Because the temperature involved in this method is significantly lower than the melting point of the base material, it is commonly used for welding of similar and dissimilar materials, whether secondary phases occur or not (Mori and Abe Ahn et al.). The heat produced by stirring the non-consumable rotating tool used for metal bonding. It can be used to join aluminium, copper, magnesium, lead, and steel plates. The process is environmentally friendly because no protective gases are used in the process. Fathi, Jalal, et al (Fathi) observed that tool tilt angle has an effect on all three responses, positively influencing tensile strength, yield strength, and percentage elongation. Tensile strength of 210 MPa, yield strength of 203 MPa,

and percent elongation of 12 were recorded using a tool with a shoulder diameter of 18mm, a 0mm offset, and a 1° tilt angle (Kumar, M, and Ramana Gao Chen).

Hassan, Malik, et al. (Hassan) investigated the effect of tool tilt angle on the mechanical properties of dissimilar aluminum and copper alloys at 0, 1, 2, 3, and 4° tilt angles. The results showed that defect-free joints were produced with a high joint strength of 117 MPa and hardness of 181VHN at the nugget area at a tool tilt angle of 4 degrees. Ahn, J., et al. (Ahn) successfully welded 6.45 mm thick 5086H32 aluminum alloys using TIG, MIG, and FSW processes, and the results showed that FSW joints had better tensile properties than fusion welded joints. Hasan, Mohammed M., et al. (Hasan) investigated the tensile strength of the dissimilar joint (AA2014 & AA6082) and con-

cluded that low rotational speed, lower travel speed, and lower tilt angle give more tensile strength. The ideal variables were 600rpm rotational speed, 60mm/min welding speed, and a 1° tilt angle. The optimum parameters where high impact value on characterization results were obtained (Kumar, M, et al. Mugada, Adepu, et al.).

Dinesh et al. investigated the greater tensile strength of (AA7075&AA6082) of 217 MPa and reported that medium rotational speed, lower welding speed, and tilt angle were all important factors (Thilagham, Muthukumaran, et al.). It increases the tensile strength of the upper and lower values. The ideal settings are 900 rpm rotational speed, 90 mm/min welding speed, and a tilt angle of 2°. From the aforementioned literature review, it is obvious that the FSW method may be applied to different alloys, and that investigations on dissimilar FSW of AA5083 and AA6082 may be carried out using a constant process parameter (Chander Grover and Singh Sharma).

Previously Khorramian, Koosha, (Khorramian and Sadeghian), investigated fusion welding of AA5083, whereas Mahendrakumar Madhavan. (Selvaraj and Madhavan) and Saravanakumar, R, et al (Saravanakumar et al.), were investigated FSW optimization and defect minimization on this 5083-H321 armor grade alloy. Similarly, the optimization and investigation of process parameters for defect-free with better mechanical and metallurgical qualities joint is investigated here. The impact of process parameters on the mechanical properties of dissimilar FSW welds of AA5083&AA6082, which are often used in shipbuilding, was investigated in this study.

2. Materials and Methods

Dissimilar aluminium alloy plates (AA6082 & AA5083) are made to the specified dimensions (100X50X6 mm³). The Chemical composition and mechanical properties of AA5083 and AA6082 in are listed in Tables 1. and Table 2. Proper tool material selection is necessary for a high-quality weld. As illustrated in Figure 1, Tool Design and Dissimilar samples of high-speed steel with a cylindrical pin profile tool was employed in this study. Following the completion of the welding using the FSW-3T-Hydraulic milling machine, the samples were prepared for tensile testing using EDM wire cut in con-

formity with applicable standard. The Tensile Failure AA6082/AA5083 samples are shown in Figure 2.

The studies are then carried out to determine the optimal working level of Process Parameters in Table 3. shows the values that were observed in experiments. To improve mechanical properties, the AA6082 is on the advancing side and the AA5083 is on the retreating side. Table 4. shows the Design of experiment for Taguchi L9 orthogonal array for welding AA6082 and 5083.

The tensile testing on the UTM machine was then characterized according to the ASTM E8/E8M-09 standard. The samples were also etched for 15 seconds with Keller's reagent (190ml water, 5ml HNO₃, 3ml HCL, and 2ml HF) to examine the microstructure and microhardness of the welds in different zones.

3. Result and Discussion

3.1. Ultimate Tensile Strength

The Tensile test result of AA6082/AA5083 Friction Stir Welded Samples is shown in Table 5. The Tensile Failure of AA6082/AA5083 samples is shown in Figure 2. Rotational speed 1200rpm, travel speed 120mm/min; tilt angle (1°) yielded a maximum tensile value of 207.49 MPa. Tensile failure was seen in the joints on AA6082 of the weld, and HAZ due to excessive heat liberation on the advancing side. The tensile failure of the tool tilt 0° AA6082/AA5083 welds is on the AA5083 of the weld, due to tunnel faults on the retreating side of AA5083.

3.2. Taguchi Analysis

The Taguchi L9 orthogonal technique was used to improve the parameter for friction stir welds AA6082/AA5083. The optimized parameter and plot graph on mean and SN/ratio are presented below.

3.2.1. Taguchi Analysis: Tensile strength (MPa versus Rotational Speed, Travel Speed, Tilt Angle)

The tensile strength response of AA6082/AA5083 is shown in Table 6. and the Main effects plot for SN Ratios and Means are shown in Figure 3. The response table for signal to noise ratios for larger is better demonstrates that tilt angle has the greatest influence on tensile strength, followed by rotational speed, and then travel speed. The findings revealed revealed that rotating speed of 1200 rpm,

TABLE 1. The Chemical Composition of AA5083 and AA6082 in W t. %

Materials	Si	Fe	Cu	Mn	Mg	Cr	Zn	Ti	Al
AA5083	0.4% max	0.4% max	0.1% max	0.4-1.0%	4.0-4.9%	0.005-0.25%	0.25% max	0.15% max	Bal.
AA6082	0.7-1.30%	0.5% max	0.1% max	0.4-1.0%	0.6-1.2%	0.25% max	0.20% max	0.10% max	Bal.

TABLE 2. The Mechanical properties of AA5083&AA6082

Properties	AA5083	AA6082
Tensile strength	305 MPa	140-330 MPa
Yield strength	195 MPa	MAX 301 MPa
Elongation at break	23%	14%
Vickers Hardness (HV)	75 HV	100HV

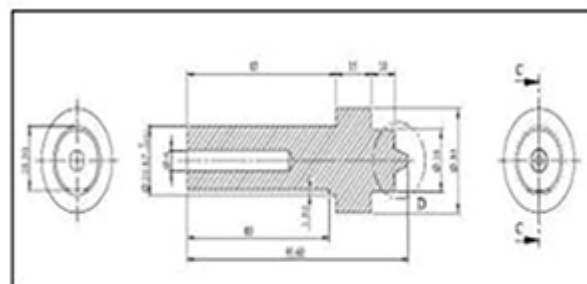


Figure 1a. Tool Design

TABLE 3. Process Parameters

FACTORS	Level-1	LEVEL-2	LEVEL-3
Rotational speed(rpm)	600	900	1200
Travel speed(mm/min)	60	90	120
Tilt angle (°)	0	1	2

TABLE 4. Design of experiment for Taguchi L9 orthogonal array

Sam-ple No.	Rotational speed (rpm)	Travel speed (mm/min)	Tilt angle (°)
1	600	60	0
2	600	90	1
3	600	120	2
4	900	60	1
5	900	90	2
6	900	120	0
7	1200	60	2
8	1200	90	0
9	1200	120	1

travel speed of 120 mm/min, and tilt angle of 1° resulted in increased tensile strength.

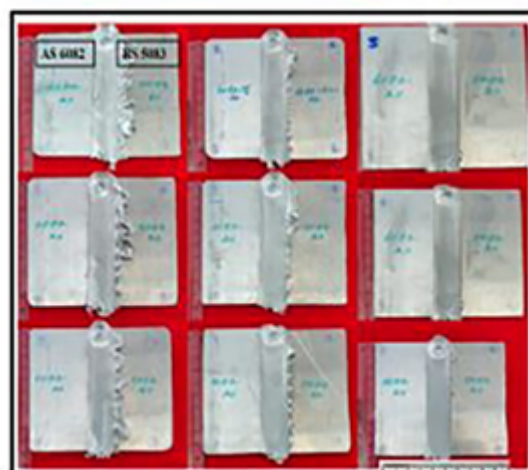


Figure 1b. Dissimilar FSW AA6082/AA5083 Samples

FIGURE 1. Tool Design (b) Tool Design & Dissimilar Samples

3.2.2. Taguchi Analysis: Yield stress (MPa versus Rotational Speed, Travel Speed, Tilt Angle

The Yield Strength Response of AA6082/AA5083 for SN Ratio and Mean is shown in Table 8 & 9, and the Main effects plot of the Yield Strength Response of AA6082/AA5083 for SN ratio and Mean are shown in Figures 4 [a,b]. The response table for signal to noise ratios for greater is better clearly illustrates that tilt angle has the greatest influence on yield strength, followed by rotational speed, and then travel speed. The Figure depicts that higher yield strength was found on rotational speed 900 rpm, travel speed 60 mm/min, and tilt angle 1°.

TABLE 5. Tensile test result of AA6082/AA5083 Friction Stir Welded Samples

S. No	Rotational speed (rpm)	Travel speed (mm/min)	Tilt angle (°)	Tensile strength (MPa)	Yield stress (MPa)	% Weld Strength Efficiency	Fracture location
1	600	60	0	115.90	96.07	13.4838%	WELD 5083
2	600	90	1	197.51	147.27	20.8860%	HAZ 6082
3	600	120	2	189.66	141.32	13.4858%	WELD 6082
4	900	60	1	195.10	179.23	13.4860%	WELD 6082
5	900	90	2	205.56	169.96	15.8063%	WELD 6082
6	900	120	0	120.07	98.32	14.9039%	WELD 5083
7	1200	60	2	203.68	169.85	9.56 62%	HAZ 6082
8	1200	90	0	113.57	94.76	13.4837%	WELD 5083
9	1200	120	1	207.49	117.15	15.8063%	HAZ 6082



FIGURE 2. Tensile Failure AA6082/AA5083 Samples

TABLE 6. Tensile strength Response of AA6082/AA5083 for Signal to Noise ratio.

Level	WS	TS	TA
1	44.25	44.42	41.33
2	44.55	44.43	46.02
3	44.54	44.50	46.00
Delta	0.30	0.07	4.69
Rank	2	3	1

TABLE 7. Tensile strength Response of AA6082/AA5083 for Mean.

Level	WS	TS	TA
1	167.7	171.6	116.5
2	173.6	172.2	200.0
3	174.9	172.4	199.6
Delta	7.2	0.8	83.5
Rank	2	3	1

TABLE 8. Yield strength Response of AA6082/AA5083 for SN ratio.

Level	WS	TS	TA
1	42.01	43.11	39.68
2	43.18	42.50	43.27
3	41.84	41.41	44.07
Delta	1.34	1.70	4.39
Rank	3	2	1

3.2.3. Taguchi Analysis: Elongation (% versus Rotational speed, travel speed, tilt angle

The % elongation response of AA6082/AA5083 for SN ratio and Mean is shown in Table 10 & 11, and the main effects of the percent elongation response of AA6082/AA5083 for SN ratio and Mean are shown in Figures 5 [a, b]. The response table for

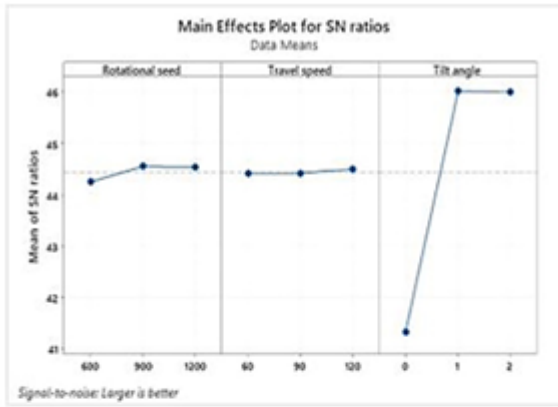


Figure 3a. Main Effects plots for SN ratios

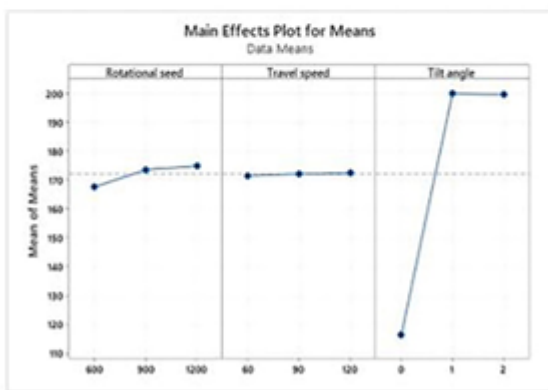


Figure 3b. Main effects plot for means

FIGURE 3. Main effects plot for (a) SN ratio (b) means

TABLE 9. Yield strength Response of AA6082/AA5083 for Mean.

Level	WS	TS	TA
1	128.22	148.38	96.38
2	149.17	137.33	147.88
3	127.25	118.93	160.38
Delta	21.92	29.45	63.99
Rank	3	2	1

signal to noise ratios for greater is better clearly illustrates that travel speed has the greatest influence on percent elongation, followed by tilt angle, and then rotational speed. The graph demonstrates that higher elongation was found on rotational speed 600 rpm, travel speed 90 mm/min, and tilt angle 1°.

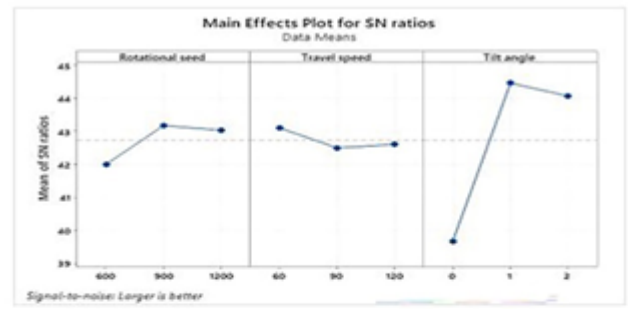


Figure 4a. Main Effects plots for SN ratios

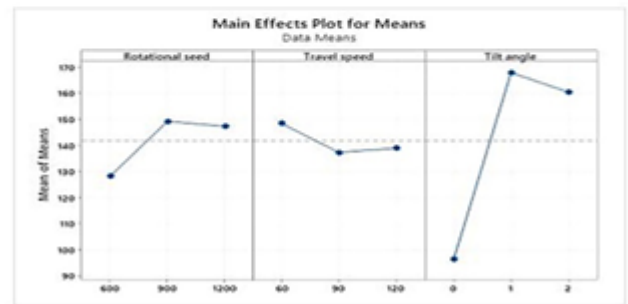


Figure 4b. Main effects plot for means

FIGURE 4. Main effects plot of the Yield Strength Response of AA6082/AA5083 for(a) SN ratios (b)Means

TABLE 10. %Elong. Response of AA6082/AA5083 for SN ratio.

Level	WS	TS	TA
1	23.86	21.60	22.88
2	23.34	24.32	24.32
3	22.06	23.34	22.06
Delta	1.80	2.72	2.26
Rank	3	1	2

TABLE 11. %Elong. Response of AA6082/AA5083 for Mean.

Level	WS	TS	TA
1	15.95	12.17	13.95
2	14.73	16.72	16.72
3	12.95	14.73	12.95
Delta	3.00	4.55	3.77
Level	WS	TS	TA

3.3. Discussion

With the aid of software Minitab21, the optimum parameters of AA6082/AA5083 friction stir welds SNL - “Larger is better” case is determined using

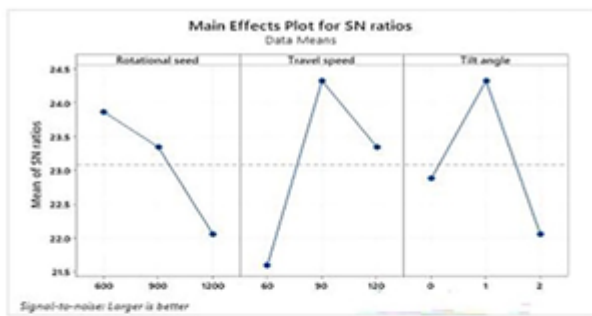


Figure 5a. Main Effects plots for SN ratios

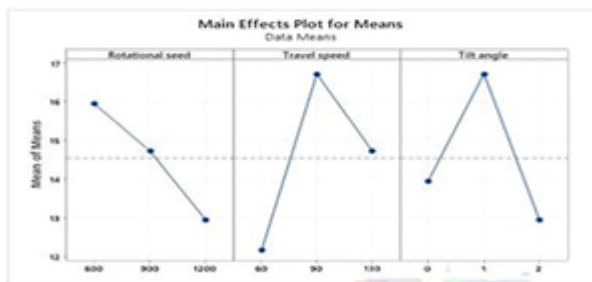


Figure 5b. Main effects plot for means

FIGURE 5. The main effects of the percent elongation response of AA6082/AA5083 for (a) SN ratios (b) Means

the following equation.

$$\frac{S}{N} = 10 \log\left(\frac{\sum (\frac{1}{Y^2})}{n}\right) \dots\dots\dots (i)$$

Where, Y is the experiment at the test and n is the total number of trials in the test. Finally, Table 13 is showing the Optimum Parameter values for the AA6082/AA5083 weld in terms of Maximum Tensile Strength, Maximum Yield Strength and Maximum Elongation.

TABLE 12. The Optimum Parameters for UTS, YS, and %E

	Rotational speed (rpm)	Travel speed (mm/min)	Tilt angle (°)
Ultimate tensile strength (MPa)	1200	120	1
Yield strength (MPa)	900	60	1
% Elongation	600	90	1

3.4. Microstructure

Figure 6a. is showing the Microstructure of AA6082 & AA5083 at 600rpm, 60mm/min, 0° degree dissimilar friction stir welded. Similarly Figure 6b is showing microstructure of AA6082 & AA5083 at 600rpm, 90mm/min, 1, Figure 6c is showing microstructure of AA6082 & AA5083 at 900rpm, 60mm/min, 1, and Figure 6d. is showing Microstructure of AA6082 & AA5083 at 1200rpm, 120mm/min, 1 correspondingly.

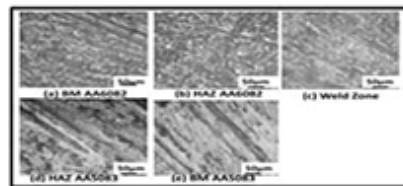


Figure 6a. Microstructure of AA6082 & AA5083 at 600rpm, 60mm/min, and 0°

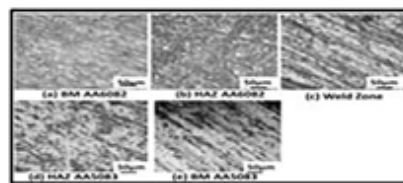


Figure 6b. Microstructure of AA6082 & AA5083 at 600rpm, 90mm/min, 1°

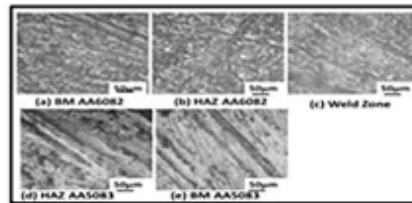


Figure 6c. Microstructure of AA6082 & AA5083 at 900rpm, 60mm/min, 1°

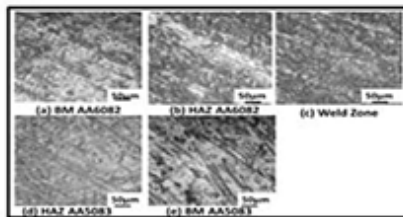


Figure 6d. Microstructure of AA6082 & AA5083 at 1200rpm, 120mm/min, 1°

FIGURE 6. Microstructure of AA6082 & AA5083 at (a) 600rpm , 60 mm/min, and 0°(b) 600 rpm , 90 mm/min, and 1°, (c) 900 rpm , 60 mm/min, and 1°, (d) 1200 rpm , 120 mm/min, and 1°

Tarmizi, Tarmizi, et al. (Tarmizi, Wahid, and Irfan), characterisation studies on AA6082/AA7075 and AA6082/2014 joint. On AA6082BM, the microstructures reveal α-solid solution of aluminum-magnesium-silicon with its intermetallic, whereas on non-heat treatable AA5083BM,

the microstructures indicate α -solid solution of aluminum-magnesium solid solution with its intermetallics. The AA6082HAZ and AA5083HAZ represent coarse grains, whereas the weld zone represents refined and recrystallized grains.

3.5. Macro Examination

The Macrostructure of FSW samples i.e., AA6082/5083 welds is shown in Figure 7. The macrostructure of several zones such as base metal, HAZ, TMAZ, and Stir zone was demonstrated. On the advancing side, the weld nugget has a basin shape, whereas on the retreating side, it has a flash projection.

3.6. Microhardness

Table 13. shows the Hardness Profile of FSW AA6082&AA5083 and Figure 8. Shows Hardness survey of samples AA6082&AA5083 measured for several weld specimens in various zones. The high microhardness of 90.5 HV attained in the different AA6082 and AA5083, which have a rotational speed of 1200rpm, a travel speed of 120 mm/min, and a tilt angle of 1°, respectively. While the tilt angles were 1° and 2°, the hardness values in AA6082HAZ decreased, and tensile failures were observed. Moreira et al., reported with the lower hardness in AA6082HAZ in AA6061/AA6082 weld. Similarly, there was a drop in harness when tilt angles were 0° at the AA5083WN weld zone were seen.

3.7. Weld Defects

3.7.1. Tunnel Defect

Figure 8. depicts the Tunnel Defects in weld samples at 0°. Tunnel flaws arise when the welding parameter is set to 0° tilt angle. The instability of the plastic deformation during the tool’s entry into the body of the work piece material at the entry zone is the main cause of the tunnel flaw. The 0°

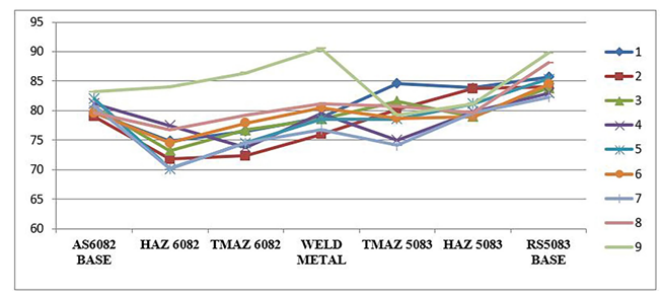


FIGURE 8. Hardness Survey of Samples AA6082 & AA5083

tilt angle is perpendicular to the workpiece surface, and extremely plastic embedding occurs as a result of material ejection as slip in the weld entry zone, leaving a tunnel defect in the area of material loss.

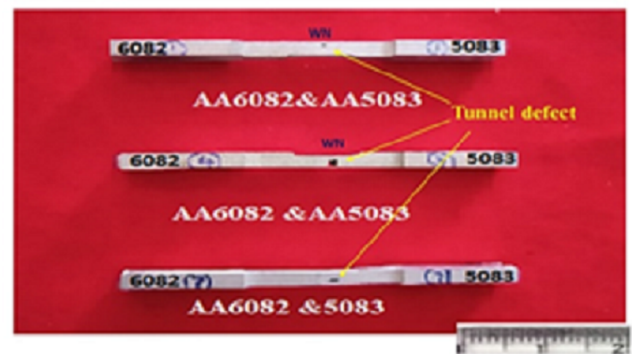


FIGURE 9. Tunnel Defect in Weld Samples

4. Conclusion

The friction stir welding of dissimilar AA6082-T6 and AA5083 H-111 was successfully completed under the impact of welding conditions, and the following interferences were drawn. Dissimilar aluminium alloys AA6082 (advancing side) and AA5083 (retreating side) have been welded using friction stir welding. At a tool rotational speed of 1200 rpm, a travel speed of 120 mm/min, and a tilt angle of 1°, the highest tensile strength of 207.49 MPa was achieved. At a tool rotational speed of 1200rpm, a travel speed of 90mm/min, and a tilt angle of 0°, the lowest tensile strength of 113.5 MPa was observed. At dissimilar welds, the tensile strength was found to be 150.71 MPa (Advancing side AA5083 & Retreating side AA6082). The higher tensile strength was 207.70 MPa on a similar weld of (AA6082& AA6082). On the advancing and retreating sides of the base metal areas, the microstructure exhibits -solid solutions of AA6082

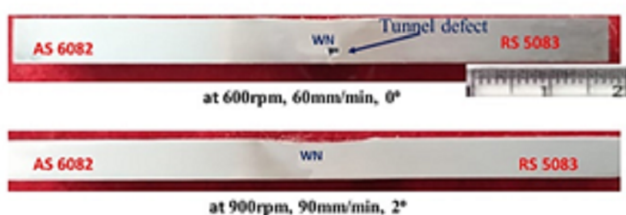


FIGURE 7. Macrostructure of FSW samples

TABLE 13. Hardness Profile of FSW AA6082&AA5083

S.NO	AS 6082 BASE	HAZ 6082	TMAZ 6082	WELD METAL	TMAZ 5083	HAZ 5083	RS5083 BASE
1	79.6	74.9	76.5	70.5	84.6	83.9	85.7
2	79	71.8	72.3	76	80.2	83.7	84.1
3	80.6	73.2	76.7	78.6	81.6	79	83.9
4	81.2	77.5	73.8	79.5	75	79.8	83
5	82	70.1	74.5	78.6	78.6	81.2	85.4
6	79.6	74.5	77.9	70.5	78.7	79	84.5
7	80.8	70.1	74.5	76.8	74.1	79.6	82.3
8	79.6	76.8	79.2	71.2	80.7	79.6	88.1
9	83.2	84	86.4	90.5	79.3	81.2	89.8

and AA5083 along with their intermetallic. The microhardness of the weld zone in a dissimilar joint with weld parameters of rotational speed 1200 rpm, travel speed 120 mm/min, and tilt angle 1° is 90.5 HV, which is greater than either AA6082BM or AA5083BM. When welding settings of tilt angle 0° was applied, tunnel defects and tunnel voids appeared on the retreating side of the AA5083 weld.

5. Future Work

SEM analysis, XRD and Corrosion studies in immersion testing of electrochemical corrosion for dissimilar joints are planned to conduct in future.

Data Availability Statement

All data that support the findings of this study are included within the article (and any supplementary files)

ORCID iDs

Mullaiarasu R.  <https://orcid.org/0000-0001-7768-0057>

References

Ahn, J. “FEM Prediction of Welding Residual Stresses in Fibre Laser-Welded AA 2024-T3 and Comparison with Experimental Measurement”. *The International Journal of Advanced Manufacturing Technology* 95.9 (2018): 4243–4263. [10.1007/s00170-017-1548-7](https://doi.org/10.1007/s00170-017-1548-7).

Ahn, Joseph, et al. “In-Situ Micro-Tensile Testing of AA2024-T3 Fibre Laser Welds with Digital Image Correlation as a Function of Welding Speed”. *International Journal of Lightweight Materials and Manufacture* 1.3 (2018): 179–188. [10.1016/j.ijlmm.2018.07.003](https://doi.org/10.1016/j.ijlmm.2018.07.003).

Chander, M Shiva. “Influence of Tool Rotational Speed and Pin Profile on Mechanical and Microstructural Characterization of Friction Stir Welded 5083 Aluminium Alloy”. *Materials Today: Proceedings* 5 (2018): 3518–3523. [10.1016/j.matpr.2017.11.599](https://doi.org/10.1016/j.matpr.2017.11.599).

Chen, L. “Microstructural and Failure Mechanism of Laser Welded 2A97 Al-Li Alloys via Synchrotron 3D Tomography”. *International Journal of Lightweight Materials and Manufacture* 1.3 (2018): 169–178. [10.1016/j.ijlmm.2018.08.001](https://doi.org/10.1016/j.ijlmm.2018.08.001).

Fathi, Jalal. “Friction Stir Welding of Aluminum 6061-T6 in Presence of Watercooling: Analyzing Mechanical Properties and Residual Stress Distribution”. *International Journal of Lightweight Materials and Manufacture* 2.2 (2019): 107–115. [10.1016/j.ijlmm.2019.04.007](https://doi.org/10.1016/j.ijlmm.2019.04.007).

Gao, Fuyang. “Microstructure and Mechanical Properties of Ti6321 Alloy Welded Joint by EBW”. *International Journal of Lightweight Materials and Manufacture* 1.4 (2018): 265–269. [10.1016/j.ijlmm.2018.08.006](https://doi.org/10.1016/j.ijlmm.2018.08.006).

Grover, Harinder and Singh. “Comparing Mechanical and Corrosion Behaviour of TIG & FSW Weldments of AA5083-H321”. *Indian Journal of Science and Technology* 10.45 (2017): 1–10. [10.17485/ijst/2017/v10i45/113537](https://doi.org/10.17485/ijst/2017/v10i45/113537).

Hasan, Mohammed M. “Effect of Pin Tool Flute Radius on the Material Flow and Tensile Properties of Dissimilar Friction Stir Welded Aluminum Alloys”. *The International Journal of Advanced Manufacturing Technology* 98.9 (2018): 2747–2758.

- Hassan, Malik. "Experimental and Numerical Simulation of Steel/Steel (St/St) Interface in Bi-Layer Sheet Metal". *International Journal of Lightweight Materials and Manufacture* 2.2 (2019): 89–96. [10.1016/j.ijlmm.2019.03.002](https://doi.org/10.1016/j.ijlmm.2019.03.002).
- Khorramian, Koosha and Pedram Sadeghian. "Material Characterization of GFRP Bars in Compression Using a New Test Method". *Journal of Testing and Evaluation* 49.2 (2019): 20180873–20180873. [10.1520/jte20180873](https://doi.org/10.1520/jte20180873).
- Kumar, Anil, H M, and V Venkata Ramana. "Influence of Tool Parameters on the Tensile Properties of Friction Stir Welded Aluminium 5083 and 6082 Alloys". *Materials Today: Proceedings* 27 (2020): 951–957. [10.1016/j.matpr.2020.01.270](https://doi.org/10.1016/j.matpr.2020.01.270).
- Kumar, Anil, H M, et al. "Optimization of Dissimilar Friction Stir Welding Process Parameters of AA5083-H111 and AA6082-T6 by CCD-RSM Technique". *Lecture Notes in Mechanical Engineering* (2018): 49–60. [10.1007/978-981-13-1724-8_5](https://doi.org/10.1007/978-981-13-1724-8_5).
- Mori, Kenichiro and Yohei Abe. "A Review on Mechanical Joining of Aluminium and High Strength Steel Sheets by Plastic Deformation". *International Journal of Lightweight Materials and Manufacture* 1.1 (2018): 1–11. [10.1016/j.ijlmm.2018.02.002](https://doi.org/10.1016/j.ijlmm.2018.02.002).
- Mugada, Kumar Krishna Kishore, Adep, et al. "Influence of tool shoulder end features on friction stir weld characteristics of Al-Mg-Si alloy". *Int. J. Adv. Manuf. Technol* 99 (2018): 1553–1566.
- Saravanakumar, R, et al. "Investigations on Friction Stir Welding of AA5083-H32 Marine Grade Aluminium Alloy by the Effect of Varying the Process Parameters". *IOP Conference Series: Materials Science and Engineering* 402.1 (2018): 12187. [10.1088/1757-899x/402/1/012187](https://doi.org/10.1088/1757-899x/402/1/012187).
- Selvaraj, Sivaganesh and Mahendrakumar Madhavan. "Investigation on Sheathing-Fastener Connection Failures in Cold-Formed Steel Wall Panels". *Structures* 20 (2019): 176–188.
- Sharma, Heena K. "Experimental Analysis of Friction Stir Welding of Dissimilar Alloys AA6061 and Mg AZ31 Using Circular Butt Joint Geometry". *Procedia Technology* 23 (2016): 566–572. [10.1016/j.protcy.2016.03.064](https://doi.org/10.1016/j.protcy.2016.03.064).
- Tarmizi, Tarmizi, R. F. A. Wahid, and I Irfan. "Effect of Welding Speed to Mechanical Properties on Friction Stir Welding of Aluminum 5052-H32". *Pengaruh Kecepatan Pengelasan Terhadap Sifat Mekanik Sambungan Alumunium Paduan 5052 Pada Proses Friction Stir Welding [Effect of Welding Speed to Mechanical Properties on Friction Stir Welding of Aluminum 5052-H32]* 34.1 (2019): 9–9. [10.14203/metalurgi.v34i1.448](https://doi.org/10.14203/metalurgi.v34i1.448).
- Thilagham, K T, S Muthukumar, et al. "Process Parameter Optimization and Characterization Studies of Dissimilar Friction Stir Welded Advancing Side AA6082-T6 with Retreating Side AA2014-T87". *Materials Today: Proceedings* 27 (2020): 2513–2519. [10.1016/j.matpr.2019.09.228](https://doi.org/10.1016/j.matpr.2019.09.228).



© R. Mullaiarasu et al. 2021 Open Access.

This article is distributed under the terms of the Creative Commons Attribution 4.0 International License (<http://creativecommons.org/licenses/by/4.0/>), which permits unrestricted use, distribution, and reproduction in any medium, provided you give appropriate credit to the original author(s) and the source, provide a link to the Creative Commons license, and indicate if changes were made.

Embargo period: The article has no embargo period.

To cite this Article: R., Mullaiarasu, Thilagham K. T., and Noorullah D.. "A Study of the Optimization and Characterization of Friction Stir Welded AA5083 and AA6082." *International Research Journal on Advanced Science Hub* 03.06 (2021): 131–139. <http://dx.doi.org/10.47392/irjash.2021.152>